THE JOURNAL OF PHYSICAL CHEMISTRY B

Article

pubs.acs.org/JPCB

# Synergistic Effect of Intramolecular Charge Transfer toward Supramolecular p$K_a$ Shift in Cucurbit[7]uril Encapsulated Coumarin Dyes

Nilotpal Barooah,[†] Mahesh Sundararajan,*[,‡] Jyotirmayee Mohanty,[†] and Achikanath C. Bhasikuttan*[,†]

[†]Radiation & Photochemistry Division and [‡]Theoretical Chemistry Section, Chemistry Group, Bhabha Atomic Research Centre, Mumbai 400 085, India

Supporting Information

**ABSTRACT:** This article presents the process and mechanism of supramolecular p$K_a$ shift in two bichromophoric coumarin laser dyes, namely, coumarin 7 (C7), ($\Delta pK_a$ = 4.6) and coumarin 30 (C30), ($\Delta pK_a$ = 3.0), achieved by introducing a synthetic macrocyclic receptor, cucurbit[7]uril (CB7), in aqueous media. The intramolecular charge transfer, from the diethylamino coumarin moiety toward the benzimidazolyl moiety and its protonation, even at pH ∼8, is facilitated by the interaction of the cucurbituril host in a 2:1 (CB7/dye) stoichiometric ratio. The CB7 macrocycle interacts with C7/C30 dyes in a stepwise manner with binding constants of the order of $K_1 \cong 10^5$ $M^{-1}$, $K_2 \cong 10^4$ $M^{-1}$ for both C7 and C30 dyes. This study underlines a structure−property relationship to explain the host induced changes in the stereoelectronic distributions in the guest dyes supporting the supramolecular p$K_a$ shifts and is appropriately established by both experimental and theoretical considerations. On the other hand, the increased solubility (>250 times) and enhancement in fluorescence intensity (>13-fold) of the coumarin dyes in the presence of CB7 also find applications for developing aqueous dye laser systems where this supramolecular strategy will largely suppress the disadvantages of low solubility, aggregation, lower emission, or low stability of the dye in aqueous medium.

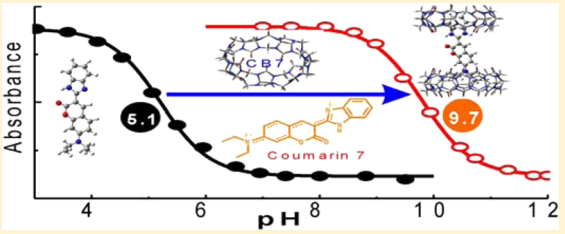


## INTRODUCTION

The encapsulation of organic molecules by preorganized hosts is often accompanied by the modification of chemical as well as physical properties of the encapsulated guests.[1−3] In the simplest case, the acid−base equilibria in appropriate guests can be modulated through encapsulation by macrocyclic synthetic receptors such as cyclodextrins, calixarenes, and cucurbiturils.[4] This phenomenon is broadly termed as supramolecular p$K_a$ shift, as the occurrence of such events is entirely governed by the formation of the host−guest systems. Among various macrocycles reported to date, owing to its dramatic effect on the acid−base equilibria of encapsulated guests, the cucurbit[*n*]uril (CB*n*) family of macrocyles is widely studied in recent years. CBs are the methylene bridged cyclic oligomers obtained from the acid catalyzed condensation of glycoluril derivatives with formaldehyde. These macrocycles have the rigid hydrophobic cavity with negatively polarized carbonyl laced portals. Because of its unique structural features, CBs interact with its guests through ion−dipole as well as hydrophobic interactions.[5] The rich host−guest chemistry of cucurbit[*n*]uril family of macrocycles was earlier reviewed by Kim[6] and Isaacs,[7] and a few more studies have appeared recently.[8−10] In particular, cucurbit[7]uril (CB7) has modest water solubility (∼5 mM in pure water),[8] which makes it an ideal host to study the various physicochemical aspects of the guests arising from their interaction with CB7. The effect of CB7 on the acid−base equilibria of the guests and its prospects as drug stabilizers and drug/prodrug carriers in pharmaceutical formulations were recently reviewed.[4,11,12] On the other hand, based on the complexation driven modulation of photophysical as well as photochemical properties of the guests, the host−guest approach has proved its utility in a wide range of applications in sensing,[13] on−off switches,[14] logic gates,[15] photostabilization,[16,17] supramolecular catalysis,[18,19] drug delivery vehicles,[20,21] enzymatic assay,[22] nanocapsules,[23] supramolecular architectures,[14,24,25] and other stimuli responsive functional devices.[26] Fluorogenic guests often respond strikingly to such complexation induced supramolecular p$K_a$ shifts because many of their photophysical aspects are intrinsically related to their chemical identity such as protonation state, structure, rigidity, etc.[12] Moreover, it is quite logical to anticipate that the stereoelectronic restrictions and the hydrophobic environment imposed by a rigid host on the guest may have pronounced effect on the protolytic equilibria of the latter inside the macrocyclic cavity. Various studies have impressively established these interconnected phenomena, and a more or less general trend of increase in basicity was observed in the case of encapsulated amine based fluorogenic guests especially with cucurbiturils.[27] Further, one of the major advantages in employing noncovalent host−guest approach is their effective

**Received:** February 21, 2014
**Revised:** May 29, 2014

   dx.doi.org/10.1021/jp501824p | J. Phys. Chem. B XXXX, XXX, XXX−XXX

and quantitative response to external stimuli such as light, environment, and exogenous ligands,[23,26,28,29] and they have been well exploited for drug carrier/delivery,[11,26] sensing,[13] or enzymatic activity/assay.[30,31] In an earlier work, taking advantage of the supramolecular p$K_a$ shift and its metal ion response, we have demonstrated the salt-induced relocation of the neutral red dye from the macrocyclic cavity of CB7 into the biomolecular pocket of bovine serum albumin.[11] Furthermore, it was also demonstrated that the encapsulation by CB7 host largely influences the well-known excited-state proton transfer processes of hydroxyphenylbenzimidazole derivatives.[32] In a recent effort, we have established a stimuli responsive supramolecular p$K_a$ shift of more than 5 pH units in the case of a coumarin dye, coumarin 6 (C6) in the presence of CB7.[33] Coumarin dyes have received much research interest in diverse areas because of their wide applicability and constitute one of the most extensively studied systems by photophysicists.[34−36] Apart from their extensive use in dye laser systems, coumarin dyes have been studied for their applications in biological systems in recent years.[37,38] Bichromophoric coumarin dyes such as coumarin 6, coumarin 7, and coumarin 30 are of particular importance for their applications as environment sensitive fluorescent probes[39−43] as well as dopents for organic light emitting diodes (OLEDs).[44,45] In these dyes, incorporation of a heterocyclic substituent at the 3-position on the coumarin core extends the electronic conjugation on the molecule as well as introduce protonation sites. Therefore, protonation/deprotonation would markedly affect the optical properties of these dyes.[40,46] The unusually large supramolecular p$K_a$ shift of C6 dye in the presence of CB7[33] prompted us to extend the study toward two other bichromophoric coumarin dyes, namely, coumarin 7 (C7) and coumarin 30 (C30) (Scheme 1). Here, we anticipated that

**Scheme 1. Structures of Cucurbit[7]uril, Coumarin 7, and Coumarin 30**

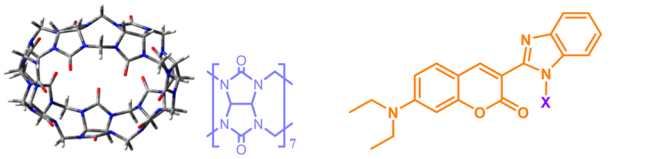


the hydrophobic microenvironment provided by the CB7 host has considerable impact on the electronic charge distribution of these coumarin dyes, which in turn plays a decisive role on their acid−base equilibrium. In this article, we report on the CB7 induced supramolecular p$K_a$ shifts in case of C7 and C30 and establish a supramolecular structure−property relationship, both experimentally and by theoretical calculations. The synergistic effect of the highly feasible intramolecular charge transfer from the diethylaminocoumarin moiety toward the benzimidazolyl moiety and the stabilizing effect of CB7 encapsulation cooperatively support large upward p$K_a$ shift of ∼4.6 pH units. Moreover, the CB7 interaction also renders the dyes more soluble, stable, and emissive in aqueous solution, a promising criteria for water-based dye laser applications.

## EXPERIMENTAL SECTION

3-(Benzimidazolyl)-7-(diethylamino)coumarin (coumarin 7, C7) and 3-(2-*N*-methylbenzimidazolyl)-7-(diethylamino)-coumarin (coumarin 30, C30) were obtained from Sigma-Aldrich and were used as received. Ethanol (spectroscopic grade) was purchased from Merck Ltd., India. Cucurbit[7]uril was synthesized according to a previously reported procedure[47] and was characterized by $^1$H NMR spectroscopy. Nanopure water (Millipore Gradient A10 system; conductivity of 0.06 $\mu$S cm$^{-1}$) was used to prepare the sample solutions. HCl/HClO$_4$ as well as NaOH used for pH adjustment was obtained from Merck Ltd., India. Solution pH was measured by pH meter model CL46+ from Toshcon Industries Ltd., India.

Ground-state optical absorption spectra were recorded in 10 mm quartz cells using a JASCO V-650 UV−vis spectrophotometer (Tokyo, Japan). Steady-state fluorescence spectra were recorded using a Hitachi (Tokyo, Japan) model F-4500 spectrofluorimeter. Since C7 and C30 were almost insoluble in water at pH > 4, for optical absorption and emission measurements, ∼10 $\mu$L of stock solution of the dyes in ethanol was added to 2 mL of Nanopure water and stirred. This solution was further diluted with water and was used for optical measurements. For measurements in acidic medium (pH 3), C7 and C30 were dissolved by sonication (∼2−3 min) in aqueous solution at room temperature. The solutions were filtered, and the filtrate was left overnight which was finally filtered again and diluted with water at pH 3, and the concentrations were evaluated using the parameters given in Note S1 in Supporting Information. For emission spectroscopy, the samples were excited at specific wavelengths to maintain minimum change in the absorbance in the presence of host and the small changes if any, have been corrected. Fluorescence quantum yields were measured by taking the reported values of C7 and C30 as benchmark ($\Phi_{f\,(30\%\ \text{ethanol−water/H+})}$ of 0.25 and 0.13, respectively).[46] Time-resolved fluorescence measurements were carried out using a time-correlated single-photon-counting (TCSPC) spectrometer (IBH, U.K.). In the present work, 445 and 451 nm diode lasers (∼100 ps, 1 MHz repetition rate) were used as the excitation source, and a microchannel plate photomultiplier tube (MCP-PMT) was used for fluorescence detection. A reconvolution procedure was used to analyze the observed decays using a proper instrument response function, and the instrument time resolution is adjudged to be better than 50 ps. The fluorescence decays were analyzed as a sum of exponentials as

$$I(t) = \sum_i B_i \exp(-t/\tau_i) \quad (1)$$

where $I(t)$ is the time dependent fluorescence intensity and $B_i$ and $\tau_i$ are the pre-exponential factor and the fluorescence lifetime for the $i$th component of the fluorescence decay.[48,49] The quality of the fits and consequently the mono- or biexponential nature of the decays were judged by the reduced $\chi^2$ values and the distribution of the weighted residuals among the data channels. The $^1$H NMR experiments were performed in $D_2O$ (99.8%) using Bruker Avance Ultrashield 700 MHz spectrometer or Varian 600 MHz Cryoprobe-HCN spectrophotometer at TIFR, Mumbai, India. The pD values of the solutions were adjusted by addition of DCl (32% in $D_2O$) to $D_2O$, and the recorded pD values were converted to pH units (+0.4).[50]

**Computational Details.** Because of the decisive role played by the noncovalent interactions in the present systems, we have carried out dispersion corrected density functional theory (DFT-D) based calculations to understand the observed supramolecular p$K_a$ shift for C7 and C30 dyes in the presence


dx.doi.org/10.1021/jp501824p | J. Phys. Chem. B XXXX, XXX, XXX−XXX

of CB7 host. In this regard, we have used BP86 functional[51,52] with def2-SV(P) basis set[53] for all atoms for geometry optimizations, whereas a B3LYP[54,55]/TZVP[56,57] (triple-$\zeta$) was used for the computation of binding and proton affinities. The above-mentioned strategy was successfully used in our earlier studies for CB and CD host–guest systems.[58] Further, to mimic the experimental conditions, we have used a continuum solvation model (COSMO) using the dielectric constant of water ($\varepsilon$ = 80). All calculations are carried out with TURBOMOLE, version 6.0.3.[59]

## RESULTS AND DISCUSSION

**Steady-State Absorption Measurements.** In neutral aqueous solution, C7 dye displays a broad absorption band centered at 450 nm (Figure 1A), much red-shifted to its

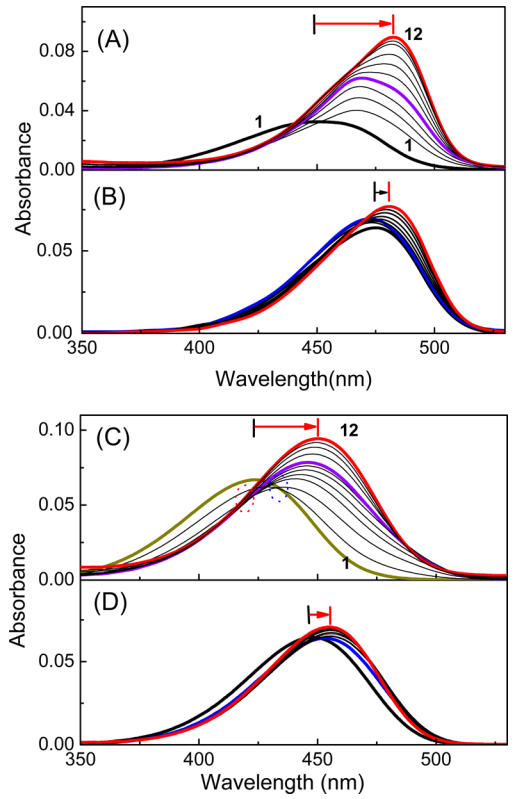


**Figure 1.** Absorption spectra of C7 (A, B). (A) 1.0 $\mu$M C7 at pH 7 with [CB7], $\mu$M: 0 (1); 5 (2); 10 (3); 17.5 (4); 37.5 (5); 67.5 (6); 110 (7); 160 (8); 260 (9); 325 (10); 412 (11); 500 (12). (B) 0.6 $\mu$M C7 at pH 3 with [CB7], $\mu$M: 0 (1); 2.5 (2); 7.5 (3); 12.5 (4); 20 (5); 30 (6); 45 (7); 65 (8); 90 (9); 125 (10); 165 (11); 215 (12). Absorption spectra of C30 (C, D). (C) 1.7 $\mu$M C30 at pH 7 with [CB7], $\mu$M: 0 (1); 10 (2); 25 (3); 50 (4); 67.5 (5); 85 (6); 110 (7); 135(8); 210 (9); 325 (10); 412 (11); 500 (12). (D) 1.1 $\mu$M C30 at pH 3 with [CB7], $\mu$M: 0 (1); 2 (2); 4 (3); 7 (4); 10 (5); 20 (6); 30 (7); 40 (8); 50 (9); 60 (10); 70 (11); 90 (12).

absorption profile in pure ethanol ($\lambda_{max}$ = 436 nm), whereas C30 dye in neat ethanol displays absorption maximum at 413 nm, which shifted to 423 nm in aqueous solution at pH 7 (Figure 1C). Recognizing the potential of the protonation equilibria in this class of dyes, we have estimated the p$K_a$ of C7 and C30 dyes in aqueous solution (containing not more than ~0.2% ethanol) by the absorption measurements (Note S2, Supporting Information). From the analysis of the variations of absorbance of C7 and C30 with respect to the solution pH (Figure S1, Supporting Information) the p$K_a$ values were estimated as 5.12 ± 0.02 and 5.02 ± 0.01, respectively, which fairly agree with earlier reports on the p$K_a$ of C7 but are slightly higher for C30 dye (reported 4.6 in 30% ethanol–water mixture).[46] From the p$K_a$ curves it is clear that at pH < 4 both dyes exclusively exist as monocations and the interaction of CB7 with C7 and C30 dyes were investigated at pH 3 and pH 7 in aqueous solution. In solution at pH 7, with incremental addition of CB7 up to 25 $\mu$M, the broad absorption band of C7 led to a hyperchromic red shift to 468 nm (Figure 1A). When CB7 concentration was increased further to about 500 $\mu$M, there was no significant change in absorption profile below 460 nm; however, the absorbance in the longer wavelengths gradually increased as a new absorption band with maximum at 482 nm (Figure 1A). On the other hand, titration of CB7 to the C30 dye at pH 7 initially displays a hypochromic red shift of the absorption profile with an isosbestic point at 432 nm. Further increase in CB7 to ~750 $\mu$M leads to gradual hyperchromic red shift of the absorption to 452 nm with a new isosbestic point at 422 nm (Figure 1C).

These absorption spectral changes for the C7 and C30 dyes at pH 7 in the presence of CB7 clearly point to a two-stage interaction of CB7 with these dyes. In the previous studies with some of monochromophoric and bichromophoric coumarin dyes, we have documented such stepwise complexation by CB7, mainly dependent on the solution pH.[33,60] Therefore, in the present cases too, it may be quite likely that apart from the 7-*N*,*N*′-diethyl group, the benzimidazole units also get encapsulated by CB7, resulting in the dramatic spectral changes. Such an interaction is expected to be more significant with the cationic forms of the dyes present at pH 3. In aqueous solution at pH 3, C7 (0.6 $\mu$M) displays absorption maximum at 475 nm (Figure 1B), assigned to the monocationic form of the dye with protonation on the benzimidazole moiety. As shown in Figure 1B, gradual increase in CB7 up to 12.5 $\mu$M resulted in a hyperchromic shift in the shorter wavelength region (below 485 nm) of the absorption profile with absorption maximum shifted to 470 nm (Figure 1B). When CB7 concentration was increased further to saturation (~165 $\mu$M), quite contrastingly, the spectrum gradually displayed a hyperchromic red shift to 480 nm with an isosbestic absorption at 466 nm (Figure 1B). These intriguing spectral changes affirm a clear two-stage interaction of CB7 with the cationic C7 dye. On the other hand, C30 at pH 3 displays absorption maximum at 446 nm assigned to the monocationic form of the dye (Figure 1D). Initial addition of CB7 (up to 7 $\mu$M) to aqueous solution of C30 (1.1 $\mu$M) resulted in a 5 nm bathochromic shift of the absorption maximum. As shown in Figure 1D, when CB7 concentration was raised further, the spectral profile showed hyperchromic shift and attained saturation in the presence of ~60 $\mu$M CB7 with an isosbestic point at 472 nm. It may be mentioned here that though the spectral changes for the cationic C30 dye are not very significant, the observed changes are in line with the changes observed at pH 7 or with that of C7 dye.

**Supramolecular p$K_a$ Shift in the Presence of CB7.** It is well-known that the interaction of aromatic amines with cucurbituril hosts increases the basicity of the amines. Therefore, the chemical identity (protonated/deprotonated state) of the guest molecule is of great importance at a specified solution pH. The bichromophoric coumarin dyes C7 and C30 consist of a benzimidazole and *N*-methylbenzimidazole unit, respectively, connected to a 7-*N*,*N*′-diethylaminocoumarin


dx.doi.org/10.1021/jp501824p | J. Phys. Chem. B XXXX, XXX, XXX–XXX

moiety. The dependence of absorption spectra of C7 and C30 dyes on the pH of the medium in the absence and presence of CB7 at the two experimental pH conditions are compared in Figure 2 along with their respective profiles in pure ethanol.

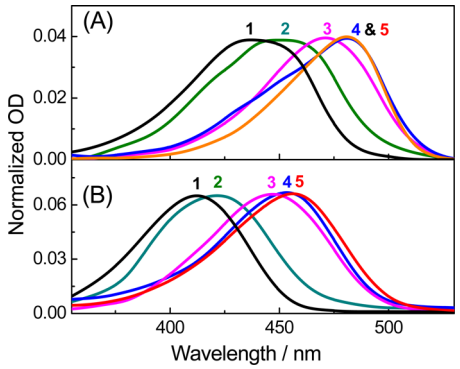


**Figure 2.** Absorption spectra of C7 (A) and C30 (B) in ethanol (1), in water at pH 7 (2), in water at pH 3 (3), with CB7 at pH 7 (4), with CB7 at pH 3 (5).

Interestingly, the absorption profile associated with C7 in the presence of CB7 (Figures 2A, 4, and 5) displays almost identical absorption maxima at pH 7 and 3. Very similarly, in the case of C30, interaction with CB7 led to almost the same changes of the absorption profile of the dye at pH 7 and 3 (Figures 2B, 4, and 5), validating the presence of protonated forms of both the dyes within the pH range of 7−3, a clear case of strong p$K_a$ shift on complexation with CB7. In separate measurements, we have ensured that the spectral changes are not due to any possible small quantities of acids associated with synthetic CB7 samples which may be capable of protonating the guest dyes. Figure 3 shows the p$K_a$ titration curves for C7

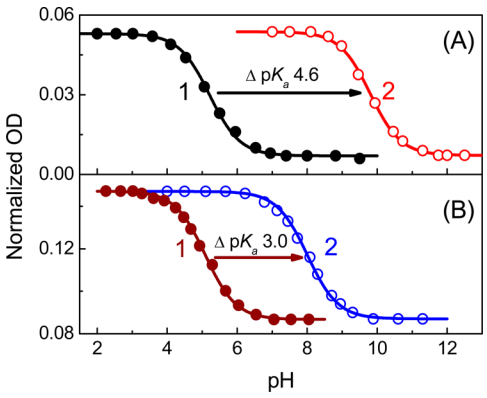


**Figure 3.** p$K_a$ titration curves for C7 (A) and C30 (B) in the absence (1) and in the presence (2) of ∼3 mM CB7.

and C30 dyes both in the absence and in the presence of CB7 (also see Note S3 and Figure S2 in Supporting Information). The estimated p$K_a$ values of C7 and C30 dyes in the presence of CB7 are 9.73 ± 0.02 and 8.02 ± 0.02, respectively, which established a supramolecular p$K_a$ shift of 4.6 and 3.0 pH units from their respective free dye values. It is intriguing to observe that in the presence of CB7, the C7 and C30 dyes remain in their cationic forms even at pH > 7.

Recently, Pluth et al. have demonstrated the possibility of performing acid catalysis in a supramolecular host under alkaline conditions, owing to its ability to protonate an included guest.[18] In another study, Nau et al. have proposed supramolecular logic following a host induced p$K_a$ shift with complexation of cucurbiturils as a supramolecular input.[15] Nevertheless, in the present case, the remarkable p$K_a$ shifts of the two structurally similar guest molecules in the presence of CB7 host may largely be dependent on the stereoelectronic properties of the guests imposed by the macrocyclic encapsulation.

**Steady-State Emission Measurements.** The emission characteristics of 7-*N*,*N*′-dialkyl substituted bichromophoric coumarin dyes are the subject of numerous investigations owing to their diverse photophysical behavior in various homogeneous and heterogeneous media. It is well established that *N*,*N*′-dialkyl substituted coumarin derivatives favor planar ICT states leading to a partially charge separated ground state, which in the excited state is highly liable to get transformed to a nonfluorescent twisted intramolecular charge transfer (TICT) state via the rotation of *N*,*N*′-dialkyl moiety with respect to the coumarin core.[34−36] Polar solvents such as water play a definite role in stabilizing such ICT character in the ground state favoring the formation of nonemissive TICT excited state, and therefore, these coumarin derivatives are weakly emissive in water.[61] Since cucurbiturils have strong affinity toward cationic guests, it is expected that CB7 will interact with the partially cationic parts of C7 and C30 dyes in the ground state, which will in turn stabilize the ICT ground state character of these dyes. In dilute aqueous solution at pH 7, C7 displays weak emission ($\Phi_{f(C7,pH7)}$ = 0.15) with maxima at around 505 nm (Figure 4A). Incremental addition of CB7 up to 25 μM to the aqueous solution of C7 (0.7 μM) at pH 7 leads to a steady increase in emission along with gradual red shift of the emission maximum to 510 nm. When CB7 concentration was increased further, emission profile registers large increase in emission without any significant shift of emission maximum, which finally saturates in the presence of ∼500 μM of CB7 (Figure 4A). It may be noted here that the emission intensity plotted at 510 nm against CB7concentration (inset, Figure 4A) displays a pseudo-saturation at ∼50 μM CB7.

On the other hand, C30 dye at neutral pH also displays weak emission with maximum at 495 nm. As shown in Figure 4C, gradual addition of CB7 to the aqueous solution of C30 at pH 7 initially displays an enhancement of the emission yield up to 85 μM CB7, which, very similar to the case of C7 dye, showed no significant increase up to 125 μM CB7. When CB7 concentration was increased further, the emission intensity increased but with a gradual red shift of emission maximum to 502 nm, reaching saturation in the presence of ∼750 μM CB7. Once again, in the case of C30 too, the emission intensity at 500 nm (inset, Figure 4C) displayed a plateau at ∼85 μM. Thus, the emission intensity changes in C7 and C30 dyes in the presence of CB7 at pH 7 clearly indicated a two-stage interaction of CB7 host with the guest dyes, very well supporting the changes recorded from the ground-state absorption measurements.

The observed emission enhancement of C7 and C30 in the presence of CB7 is attributed to the formation of inclusion complex in which the emissive species is protected inside the hydrophobic cavity of CB7. Hence it is is anticipated that at pH 3, CB7 will interact with the cationic benzimidazole or *N*-methylbenzimidazole part of C7 and C30, respectively, through strong ion dipole interaction leading to the formation of 1:1 host−guest complex. Moreover, it is quite likely that the coumarin moieties of these complexes may also interact with


dx.doi.org/10.1021/jp501824p | J. Phys. Chem. B XXXX, XXX, XXX−XXX

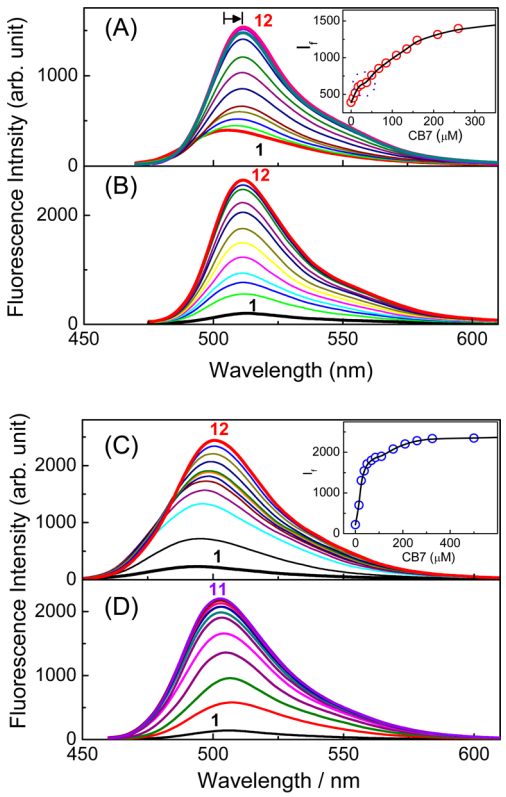


**Figure 4.** Fluorescence spectra of C7 (A, B). (A) 1.0 $\mu$M C7 at pH 7 with [CB7], $\mu$M: 0 (1); 5 (2); 10 (3); 17.5 (4); 37.5 (5); 67.5 (6); 110 (7); 160 (8); 260 (9); 325 (10); 412 (11); 500 (12). (B) 0.6 $\mu$M C7 at pH 3 with [CB7], $\mu$M: 0 (1); 2.5 (2); 7.5 (3); 12.5 (4); 20 (5); 30 (6); 45 (7); 65 (8); 90 (9); 125 (10); 165 (11); 215 (12). Fluorescence spectra of C30 (C, D). (C) 1.7 $\mu$M C30 at pH 7 with [CB7], $\mu$M: 0 (1); 10 (2); 25 (3); 50 (4); 67.5 (5); 85 (6); 110 (7); 135(8); 210 (9); 325 (10); 412 (11); 500 (12). (D) 1.1 $\mu$M C30 at pH 3 with [CB7], $\mu$M: 0 (1); 2 (2); 4 (3); 10 (4); 20 (5); 30 (6); 40 (7); 50 (8); 60 (9); 70 (10); 90 (11).

another CB7 molecule further through hydrophobic interactions leading to the formation of ternary C7/C30−CB7 complexes. In the present study we observe that C7 and C30 in their cationic forms are weakly emissive ($\Phi_{f(C7)}$ = 0.05 and $\Phi_{f(C30)}$ = 0.04) in aqueous solution which can be rationalized taking into account of the intermolecular charge transfer character of the cationic species. Figure 4B,D depicts the steady-state emission spectral profile for C7 and C30 dyes in the presence of CB7 at pH 3. In the case of C7 (~0.6 $\mu$M), addition of CB7 results in a steady increase in the emission yield with a blue shift of ~5 nm of the emission maximum to 510 nm and attains saturation in the presence of ~215 $\mu$M CB7 (Figure 4B). On the other hand, in the case of C30 dye (1.1 $\mu$M) similar measurements with CB7 leads to the saturation in emission at ~60 $\mu$M CB7 (Figure 4D). In the presence of CB7 (at saturation concentration), the quantum yields of emission of C7 and C30 in aqueous solution at pH 3 are evaluated as 0.46 and 0.52, respectively.

It may be noted that except for the emission enhancement, the significant spectral shifts observed for the dyes in the presence of CB7 at pH 7 were not observed for the titrations carried out at pH 3. This contrasting behavior led us to believe that the initial interactions of CB7 with the guest dyes are dissimilar owing to the fact that C7 and C30 dyes contain two equally probable binding sites for the host CB7. At neutral pH the partial charge-separated ground-state structures of C7 and C30 dyes place the partial positive charge on the 7-*N*,*N*′-diethylamino group of the coumarin core. Therefore, the initial interaction of CB7 with these guest dyes at pH 7 would take place through the interaction with the 7-*N*,*N*′-diethylamino group. At low concentration of CB7 this initial binding interaction displayed a pseudo-saturation level in both of the dyes, which on increase of the host concentration led to a further increase in emission with a red shift of the emission maxima. Importantly, the final emission maxima of C7 and C30 dyes with CB7 at pH 7 closely match that at pH 3 (Figure 4) and corroborate the absorption spectral changes and the supramolecular p$K_a$ shifts discussed before (also see the theoretical discussions in the later part).

It is apparent from Figure 3 that the study of the interaction of the neutral forms of the dyes with CB7 need to be carried out at pH > 10 to ensure the respective neutral forms of the dyes, even after CB7 interaction. Though C7 dye is chemically unstable at pH ~ 10 (Note S4(A), Figure S3, Supporting Information), the C30 dye is found to be relatively stable at pH 10.5 (5 mM bicarbonate buffer). Unlike the spectral changes observed for a clear 1:1 and 2:1 (CB7/C30) stoichiometric composition at pH 7 and 3, the prominent changes observed in the absorption and emission spectra of C30 dye at pH 10.5 represent the presence of both stoichiometries. Detailed spectroscopic changes are discussed in Note S4(B), Figure S3 (Supporting Information), and the photophysical parameters are included in Table 1. In a separate experiment we have verified that the emission intensities of these dyes are stable and reproducible on cyclic change in the solution pH from 3 to 10.

**Table 1. Absorption and Fluorescence Characteristics of C7 and C30 Dyes with CB7 at Different pH Conditions in Aqueous Solutions**

| pH | [CB7] ($\mu$M) | $\lambda_{max}^{abs}$ (nm) | $\lambda_{max}^{em}$ (nm) | $\Phi_f$ | $\tau_1$ (ns) (% $a_1$) | $\tau_2$ (ns) (% $a_2$) |
|---|---|---|---|---|---|---|
| Coumarin 7 (C7) Dye | | | | | | |
| 3 | 0 | 471 | 512 | 0.05 | 0.15 (97) | 1.18 (3) |
| 3 | 390 | 481 | 511 | 0.46 | 0.38 (11) | 1.90 (89) |
| 7 | 0 | 453 | 505 | 0.15 | 0.15 (6) | 1.22 (94) |
| 7 | 50 | 468 | 509 | | 0.52 (12) | 2.87 (88) |
| 7 | 500 | 481 | 511 | 0.489 | 0.42 (12) | 2.11 (88) |
| Coumarin 30 (C30) Dye | | | | | | |
| 3 | 0 | 447 | 506 | 0.042 | 0.13 (100) | |
| 3 | 500 | 456 | 507 | 0.52 | 0.69 (18) | 2.06 (82) |
| 7 | 0 | 423 | 494 | 0.098 | 0.12 (18) | 0.39 (82) |
| 7 | 50 | 440 | 498 | | 0.41 (8) | 3.02 (92) |
| 7 | 500 | 453 | 503 | 0.51 | 0.69 (15) | 2.16 (85) |
| 10.5 | 0 | 422 | 494 | 0.097 | 0.31 (100) | |
| 10.5 | 425 | 435 | 493 | 0.74 | 0.35 (5) | 2.90 (95) |

**Excited-State Decay Kinetics.** Earlier reports reveal that the excited-state decay kinetics of such bichromophoric coumarin dyes show exceptionally high nonradiative decay rates in highly polar protic solvents.[40,62,63] Moreover, it was shown that while the excited-state deactivation mainly occurs through the ICT to TICT conversion, the actual activation controlled rate-determining step for effective nonradiative process is the TICT state to ground state conversion in polar protic solvent medium.[39] The formation of TICT states in 7-dialkylamino substituted coumarins involves the rotation of the *N*,*N*′-dialkyl substituent with respect to the coumarin moiety


dx.doi.org/10.1021/jp501824p | J. Phys. Chem. B XXXX, XXX, XXX–XXX

during the excited-state lifetime of the dyes. As stated earlier, factors that can impose restriction on intramolecular rotation will disfavor the formation of the nonemissive TICT state and thereby enhance the radiative emission probability with increase in the excited-state lifetime. With this argument it is anticipated that the encapsulation of 7-*N*,*N*′-diethylamino coumarin group of C7 and C30 dyes inside the hydrophobic cavity of CB7 should increase their excited-state lifetimes. The comparative decay profiles of C7 and C30 in free and in the presence of CB7 under various experimental conditions are shown in Figure 5, and the lifetime values are provided in Table 1. The decay traces and the time constants for each set of experiments carried out at specific solution pH are detailed in the Supporting Information (Figure S4, Table S1). At pH 3, C7 displays fast decay kinetics with a lifetime of 0.15 ns and a negligible contribution from a relatively longer decay component, manifesting the intramolecular charge transfer character of the monocationic form of C7 in the excited state.

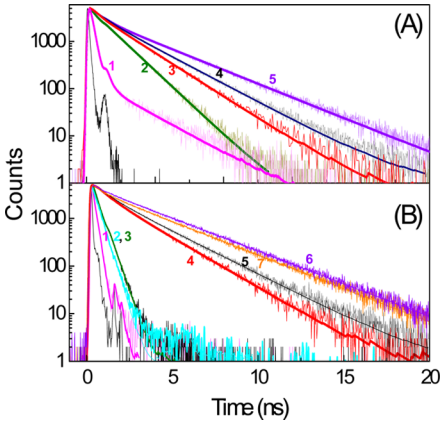


**Figure 5.** Fluorescence decay traces (A) of C7 (~1 $\mu$M) in water at pH 3 (1), in water at pH 7 (2), with CB7 at pH 3 (3), with CB7 (500 $\mu$M) at pH 7 (4), and with CB7 (50 $\mu$M) at pH 7 (5) and (B) of C30 (~1.5 $\mu$M) at pH 3 (1), pH 7 (2), pH 10.5 (3), with CB7 at pH 3 (4), with CB7 (500 $\mu$M) at pH 7 (5), with CB7 in 5 mM bicarbonate buffer at pH 10.5 (6), with CB7 (50 $\mu$M) at pH 7 (7). $\lambda_{ex}$ = 451 nm. $\lambda_{em}$ = 520 nm.

On the other hand, at pH 7, excited-state decay is mainly governed by a longer decay component of 1.2 ns as well as a minor contribution from a short component of 0.15 ns (Table 1). With increasing concentration of CB7, the excited state decay of cationic C7 dye (pH 3) displayed a gradual increase in lifetime (Figure S4, Supporting Information), and with ~390 $\mu$M CB7, the biexponential decay provided a major component of 1.9 ns (89%) with minor component of 0.38 ns (11%) (Figure 5). Considering that the initial encapsulation of C7 occurs at the cationic benzimidazole unit and then at the *N*,*N*′-diethylaminocoumarin unit, the lifetime components of 0.38 and 1.9 ns are attributed to the 1:1 and 2:1 (CB7/C7) stoichiometries, respectively.

At pH 7, the initial interaction of CB7 is at the *N*,*N*′-diethylaminocoumarin unit, followed by the encapsulation of the benzimidazole unit with concomitant protonation. From Table 1, it can be clearly seen that the initial complexation of the *N*,*N*′-diethylaminocoumarin unit is associated with the increase in lifetime of the excited state to 2.8 ns, which in the presence of high CB7 concentration decreases to 2.1 ns. Note that the decay profile in the presence of CB7 at pH 7 approaches the decay recorded at pH 3 with CB7, further substantiating the CB7 assisted supramolecular p$K_a$ shift in C7 dye.

Similarly, the complexation sequence of CB7 with C30 at different pH conditions could be clearly judged from the excited-state lifetime values provided in Table 1. Very similar to the C7 dye, C30 also displays fast excited-state decay kinetics in acidic aqueous media at pH 3, and the decay is relatively slower (0.3−0.4 ns) in solutions at pH 7. In the presence of increasing concentrations of CB7 host the cationic C30 dye (pH 3) displays a gradual increase in lifetime up to 2 ns, attributed to the 2:1 (CB7−C30H$^+$) ternary complex along with a minor component of ~0.7 ns which could be the characteristic of the 1:1 (CB7−C30H$^+$) complex (Figure S5, Table S2). On the same line, the neutral form of the dye at pH 10.5 displays slower decay kinetics in the presence of CB7 and the estimated lifetime is ~2.9 ns (see Note S5, Figure S6, and Table S3 in Supporting Information).

**$^1$H NMR Studies on Interaction of C7 and C30 Dyes with CB7.** The interaction of C7 and C30 dyes with CB7 host in $D_2O$ was investigated by $^1$H NMR spectroscopic techniques at specific solution pD. In general, while the encapsulation inside the hydrophobic cavity of CB7 renders an upfield shift of the proton resonances, the protons residing in the vicinity of the negatively polarized carbonyl portals experience a strong deshielding effect and display downfield shift with respect to their parent positions in $^1$H NMR spectra. Because of insufficient solubility of C7 and C30 in aqueous media at neutral pD, NMR studies have been mainly carried out at pH 3, where they are relatively more soluble.

As shown in Figure 6, C30 dye in the presence of ~2.5 equiv of CB7 displayed considerable complexation induced upfield shifts in the *N*,*N*′-diethylaminomethyl group ($\delta$ 1.14−0.5) and the −$CH_2$ quartet from ($\delta$ 3.54−2.75), demonstrating that these protons reside in the hydrophobic shielding region of the cavity. Similarly, other protons in the methyl and aromatic positions also displayed shielding and deshielding effects, corresponding to their positioning in the CB7 cavity, and the details are discussed in Note S6, Supporting Information. $^1$H NMR studies with C7 dye in the presence of CB7 also

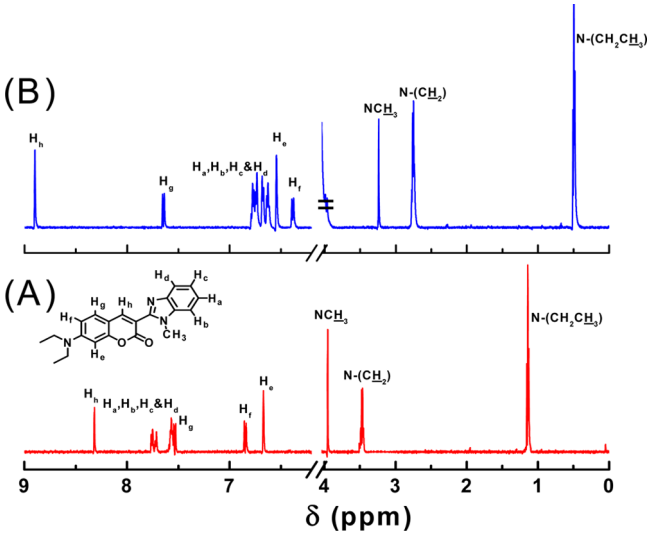


**Figure 6.** $^1$H NMR spectra of C30 in $D_2O$: at pH 3 (A); with CB7 (2.5 equiv) at pH 3 (B).


dx.doi.org/10.1021/jp501824p | J. Phys. Chem. B XXXX, XXX, XXX−XXX

displayed very similar features except the observation that the aromatic protons on the benzimidazole unit appeared as a broad multiplet in the presence of CB7 (Figure S7). Thus, it is once again verified that C7 and C30 dyes in its cationic form interacts with two CB7 host molecules through the encapsulation of the cationic benzimidazole/*N*-methylbenzimidazole unit as well as the 7-*N*,*N*′-diethylaminocoumarin unit in the hydrophobic cavity of CB7, leading to ternary $(CB7)_2$−C7 and $(CB7)_2$−C30 host−guest complexes.

**Binding Constant of C7 and C30 Dyes with CB7.** The binding constant values were evaluated from the nonlinear regression analysis of the plot of emission intensity at 520 nm with respect to CB7 concentration by considering the following two-stage complexation equilibria for 1:1 and 2:1 host−guest complexes. At pH 3

$$\text{dye} + \text{CB7} \overset{K_1}{\rightleftharpoons} \text{dye–CB7} \tag{2}$$

$$\text{dye–CB7} + \text{CB7} \overset{K_2}{\rightleftharpoons} \text{dye–(CB7)}_2 \tag{3}$$

where $K_1$ and $K_2$ are the binding constants for the formation of the respective 1:1 and 2:1 complexes. At any stage, the observed fluorescence intensity $I_f$ values correspond to the sum of the fluorescence intensities arising from the free dye, CB7−dye, and $(CB7)_2$−dye host−guest complexes and are directly proportional to their respective concentrations present in the solution.

Therefore, observed emission intensity can be expressed as

$$I_f = I_f^0\frac{[\text{dye}]_{eq}}{[\text{dye}]_0} + I_{CB7-dye}\frac{[CB7-\text{dye}]_{eq}}{[\text{dye}]_0} + I_{(CB7)_2-dye}\frac{[(CB7)_2-\text{dye}]_{eq}}{[\text{dye}]_0} \tag{4}$$

where, $I_f^0$ is the fluorescence intensity of the dye in the absence of CB7, $I_{CB7-dye}$ and $I_{(CB7)_2-dye}$ are the fluorescence intensity of the corresponding 1:1 and 1:2 complexes with CB7 in solution. Equation 4 can be rearranged to a modified Benesi−Hildebrand equation as in eq 5, which expresses the total intensity as a function of host concentration.

$$I_f = \frac{I_f^0 + I_{CB7-dye}K_1[CB7]_0 + I_{(CB7)_2-dye}K_1K_2[CB7]_0^2}{1 + K_1[CB7]_0 + K_1K_2[CB7]_0^2} \tag{5}$$

By application of eq 5 to fit the experimental data presented in Figure 7, the $K_1$ and $K_2$ values were estimated to be $(1.3 \pm 0.3) \times 10^5$ $M^{-1}$ and $(1.8 \pm 0.2) \times 10^4$ $M^{-1}$, respectively, for the binding of monocationic C7 dye with CB7 at pH 3. Similar analysis for C30 dye yields the association constant ($K_1$ and $K_2$) values as $(3.1 \pm 0.2) \times 10^5$ $M^{-1}$ and $(4.1 \pm 0.5) \times 10^4$ $M^{-1}$, respectively, at pH 3. Although the association constants for both C7 and C30 dyes with the common CB7 host are of similar order, the overall binding constant ($K = K_1K_2$) for C30 dye is slightly higher than for C7 dye in aqueous solution at pH 3. Nevertheless, the estimated binding constant values indicate a strong binding of the cationic C7 and C30 dyes with CB7 as expected for host−guest equilibria driven mainly by strong ion−dipole and hydrophobic interactions. At this point it may be noted that a similar procedure for the estimation of binding constants for C7 and C30 dyes with CB7 host may not be applicable at pH 7 because of the change of the chemical identity of the guest dyes from neutral to cationic form during the titration with CB7 host. On the other hand, at pH 10.5, the estimated binding constant is $(4.4 \pm 0.1) \times 10^4$ $M^{-1}$ which is approximately an order of magnitude lower than the 1:1 binding constant of CB7−C30 system observed at pH 3. We anticipate that the presence of millimolar concentrations of buffer apparently decreases the binding constant of coumarin dyes with CB7 at least by an order of magnitude through the competitive binding of the cations of the buffer with CB7.

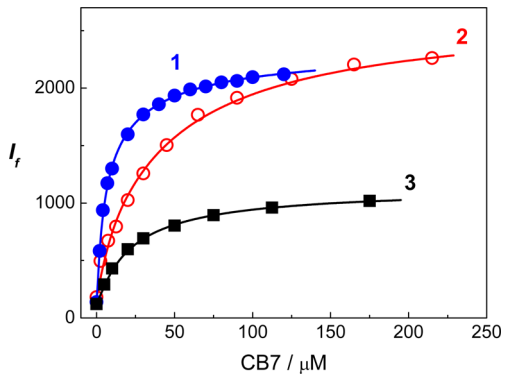


**Figure 7.** Binding isotherm of (1) C30 (1.1 $\mu$M, at pH 3), (2) C7 (0.6 $\mu$M, at pH 3), (3) C30 (1.0 $\mu$M in 5 mM bicarbonate buffer at pH 10.5) with [CB7]. Emission was monitored at 520 nm, $\lambda_{ex}$ of 470 nm for C7 and 450 nm for C30 dyes. The solid lines represent the best fitted curves according to eq 5.

**Intramolecular Charge Transfer (ICT) and CB7 Assisted Protonation.** So far we have established that C7 and C30 dyes interact with the synthetic receptor host CB7 to form 2:1 ternary host−guest complexes in neutral to acidic solutions. The encapsulation of the guest dyes by CB7 is accompanied by dramatic p$K_a$ shift of the dyes leading to CB7 stabilized cationic species existing in basic medium; e.g., p$K_a$ of C7 as $(CB7)_2$−C7 complex is 9.7. At this point it is worth mentioning that a simple benzimidazole while encapsulated inside CB7 cavity shows a p$K_a$ shift of 3.5 units and many benzimidazole-containing drug molecules show p$K_a$ shifts in the range of 2−4 units in the presence of CB7 in aqueous solution.[4] In the present case for C7 dye, where the benzimidazole unit is attached to a 7-*N*,*N*′-diethylaminocoumarin unit, it shows an unusually large p$K_a$ shift of 4.6 units. Here the benzimidazole unit is in electronic conjugation with the 7-*N*,*N*′-diethylaminocoumarin part. Therefore, we have attempted a simple structure−property relationship to explain the reason behind the large p$K_a$ shift of the guest dyes in the presence of CB7.

Various studies have established that in polar protic solvents in neutral pH, 7-*N*,*N*′-diethylamino substituted coumarin derivatives exist in a partially charge separated intramolecular charge transfer (ICT) state adopting a near planar conformation facilitating the delocalization of nonbonding electrons on dialkyl substituted nitrogen atom over the entire coumarin core, which is further stabilized by the carbonyl group and any electron withdrawing groups (e.g., $-CF_3$) on the coumarin unit.[61,63] Polarity and hydrogen bonding ability of the solvent play a decisive role in stabilizing such zwitterionic forms through effective solvation. In the cases of C7 and C30 dyes used in this study, the expected ICT state would be represented by the canonical form **III** (Scheme 2) where the benzimidazole substitution at position 3 remains as a spectrator part. However, along with this one can imagine an equally probable canonical from **II** with the electronic charge delocalization over the benzimidazole unit. Although the electronegativity of oxygen is higher than nitrogen, the resonance structure **II** will be predominatly contributing because of the delocalization of


dx.doi.org/10.1021/jp501824p | J. Phys. Chem. B XXXX, XXX, XXX−XXX

**Scheme 2. Canonical ICT Structures of C7 and C30 Dyes at Neutral pH**

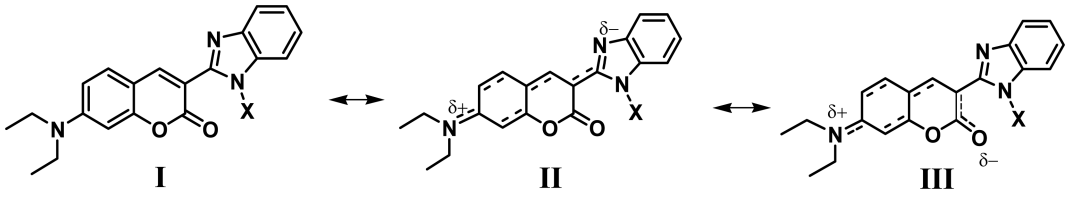

partial negative charge over the aromatic benzimidazole unit. In this ICT form of the guest dyes, CB7 interacts with the partially positive 7-*N*,*N*′-diethylaminocoumarin unit at neutral pH. Encapsulation of 7-*N*,*N*′-diethylamino substituent inside the cavity of CB7 further stabilizes the ICT form of the dye which invariably increases the probability of protonation on the benzimidazole nitrogen atom. Therefore, it is anticipated that depending on the proton concentration in solution, benzimidazole units on the CB7 bound dyes as 1:1 host−guest complex get protonated at much higher pH compared to free dye. The binding of the second CB7 host through the encapsulation of the protonated benzimidazole units is absolutely necessary to stabilize the protonated form of the dye in the respective solution pH, and these two effects operate synergistically. In other words, the deprotonation of the cationic guests in the 2:1 ternary complexes with CB7 becomes significantly difficult, and so the p$K_a$ is higher. The proposed hypotheses on binding of CB7 and its effect on the acid base equilibria are further substantiated by the absorption and emission spectroscopic changes observed for the neutral form of the dye in the presence of increasing concentration of CB7 host at pH 7.

On the other hand at pH 3, C7 and C30 dyes are in cationic states with protonation on the benzimidazole nitrogen atoms and are stabilized through charge delocalization over the entire molecule as represented by two canonical structures **IV** and **V** in Scheme 3. In aqueous solution, binding of CB7 is expected

**Scheme 3. Canonical ICT Structures of C7 and C30 Dyes at pH 3**

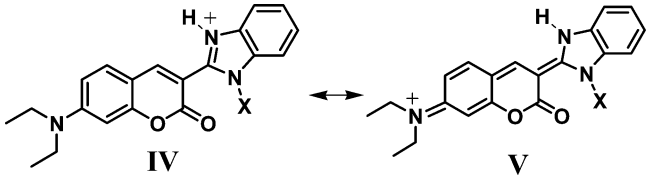

to be stronger with the positively charged dye molecules. We could not experimentally distinguish the two stages of binding of CB7 to C30 dye in acidic pH.

**Theoretical Predictions of C7 and C30 Binding to CB7.** To validate our hypotheses on the role of initial binding of CB7 to 7-*N*,*N*′-diethylamino substituent on the p$K_a$ of the electronically conjugated benzimidazole/N-methylbenzimidazole units of C7 and C30 dyes, detailed theoretical calculations were performed for the proton affinity of free dyes and complexed with CB7 in 1:1 ratio. The entire event for each dye can be represented as a cyclic process and is represented in Scheme 4, the C7 case with their geometry optimized structures.

Prior to the host−guest complexation, we have optimized the neutral and protonated dyes (C7 and C30) in various isomeric forms of the bare dye. Two geometric isomers arise with respect to the rotation of ethyl groups attached to the terminal

**Scheme 4. Protonation and Binding Processes for Neutral C7 Dyes with CB7 Based on DFT Level of Theory**

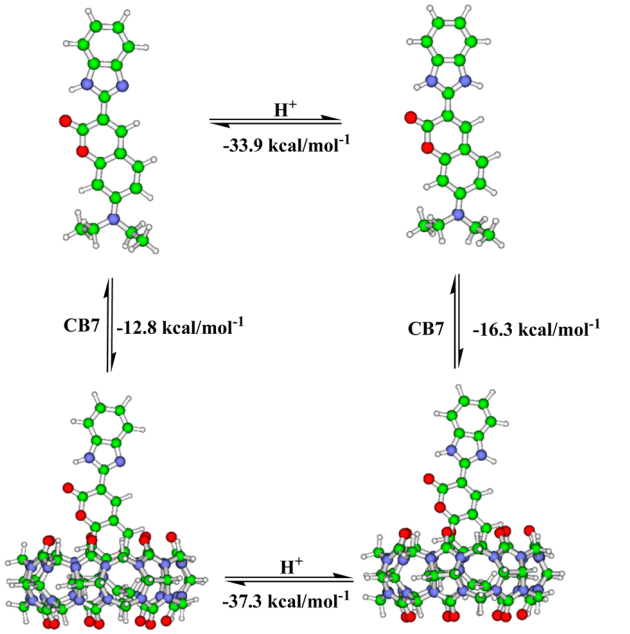


nitrogen of the dyes (Figure S8). We find that irrespective of the tail group orientations, the heterocyclic ring system is planar and both species (C7 and C30 dyes) are nearly isoenergetic (less than 0.5 kcal mol$^{-1}$). For C7 dye, a very strong hydrogen bonding (N−H···O, 2.048 Å) is noted between the proton attached to the benzimidazole moiety and the coumarin oxygen in both cis and trans isomers. Further, replacement of proton of benzimidazole moiety by methyl group (C30 dye) can exist in various conformations due to the steric hindrance present between the methyl group of benzimidazole moiety and coumarin carbonyl group. We have considered three different forms denoted as trans−cis, trans−trans, and trans−skew (Figure S8). Of the three forms, the trans−skew form is the most stable species (by 4 kcal mol$^{-1}$) because of minimal steric hindrance between the two heterocyclic rings.

Protonation of benzimidazole nitrogen of C7 dye is favored by ∼33.9 kcal mol$^{-1}$. Further, we note that the intermolecular N−H···O hydrogen bonding in C7−CB7 complex is somewhat stronger in the protonated form (1.994 Å) compared to the neutral form. However, an interesting conformational change is observed from trans−skew to trans−trans form upon protonation of the C30 dye because of favorable hydrogen bonding interaction (1.829 Å). Compared to the C7 dye, the computed proton affinity for the C30 dye is slightly larger (−35.3 kcal mol$^{-1}$) because of the electron donating nature of the methyl substituent in C30 form.

As shown in Scheme 4, the protonation on the benzimidazole nitrogen of free C7 dye is favored by 33.9 kcal


dx.doi.org/10.1021/jp501824p | J. Phys. Chem. B XXXX, XXX, XXX−XXX

mol$^{-1}$ in aqueous medium. Both the neutral and the cationic forms of C7 dye in aqueous media can form 1:1 host−guest complex with CB7 with the complete encapsulation of the 7-*N*,*N*′-diethylamino part inside the CB7 cavity as represented by the favorable binding energy of −12.8 and −16.3 kcal mol$^{-1}$, respectively. Upon encapsulation, we note that the hydrogen bonding between the benzimidazole proton and the coumarin oxygen is even stronger for both CB7-neutral (1.997 Å) and CB7-protonated dye forms (1.950 Å) compared to the free dye. Moreover, in the case of neutral form of the dye the electron density (derived from natural population analysis) on the benzimidazole nitrogen atom increases from −0.508 for the free state to −0.518 in the inclusion complex with the CB7 host. Similarly the proton affinity of C7 dye as 1:1 complex with CB7 is evaluated to be 37.3 kcal mol$^{-1}$, which suggests that the protonation process on the benzimidazole unit in the CB7 bound dye is more favorable by −3.4 kcal mol$^{-1}$ compared to its free state. It is interesting to observe that at a specific solution pH, the enhanced probability of protonation on the benzimidazole nitrogen atom occurs in a host−guest configuration where the benzimidazole unit itself is not encapsulated inside the hydrophobic cavity of CB7. Instead the CB7 host encapsulates the 7-*N*,*N*′-diethylamino group of C7 dye.[64] This observation clearly indicates the role of CB7 encapsulation in the coumarin end to the overall stereo-electronics of the molecule. As anticipated earlier, encapsulation of the 7-*N*,*N*′-diethylamino group of the coumarin end effectively stabilizes the ICT character of C7 dye and thereby increases the electron density on the benzimidazole nitrogen atom through effective charge delocalization.

Therefore, the above-described theoretical approach dictates that the canonical from **II** is equally or more probable in describing the ICT character of C7 dye in polar protic medium such as water. Finally it is pleasing to observe that the difference between the binding of neutral and the cationic C7 dye with CB7 is equal to the difference of proton affinity of the dye in free and the bound state. This observation clearly indicates the inter-relation between the binding events of CB7 host to remote coumarin end and the protonation at the distal benzimidazole unit at specific solution pH. Further, the protonated form can trigger the binding of second CB7 host molecule leading to the formation of 2:1 host−guest complex. In fact, the formation of higher stoichiometric ratio of host−guest systems was earlier reported by us for cyclodextrin−oxazine systems.[58] A very similar binding pattern and associated increase in probability of protonation was also observed for C30 dye upon encapsulation to CB7 (Figure S9).

## CONCLUSION

In short, here we report the supramolecular interaction of two bichromophoric coumarin laser dyes, namely, C7 and C30 with a macrocyclic receptor, CB7, in aqueous media at different pH conditions. The dramatic change in the stereoelectronic distribution in the dye due to the 2:1 (CB7−dye) stoichiometric complexation resulted in a large upward shift in the p$K_a$ to stabilize the protonated form even at pH ∼8. On the basis of the extensive experimental and theoretical considerations, this work establishes a structure−property relationship to explain the host induced supramolecular p$K_a$ shifts in noncovalently bound systems, a phenomenon that is of immense significance for drug delivery applications. The results discussed here also find applications for developing aqueous dye laser systems where the supramolecular strategy for a laser dye will largely suppress the practical disadvantages of low solubility, aggregation, lower emission or stability of the active dye in aqueous media. In this direction, investigations on the practical applications of CB7−C7 and CB7−C30 host−guest systems in aqueous media are in progress.

## ASSOCIATED CONTENT

### Supporting Information

Molar extinction coefficients, p$K_a$ data, absorption spectra, lifetime measurements, $^1$H NMR spectra, and geometry optimized structures. This material is available free of charge via the Internet at http://pubs.acs.org.

## AUTHOR INFORMATION

### Corresponding Authors

*M.S.: e-mail, smahesh@barc.gov.in (correspondence for the theoretical part only).

*A.C.B.: e-mail, bkac@barc.gov.in.

### Notes

The authors declare no competing financial interest.

## REFERENCES

(1) Brinker, U. H.; Mieusset, J.-L. *Molecular Encapsulation: Organic Reactions in Constrained Systems*; John Wiley & Sons, Ltd.: Chichester, U.K., 2010.

(2) Hof, F.; Craig, S. L.; Nuckolls, C.; J. Rebek, J. Molecular Encapsulation. *Angew. Chem., Int. Ed.* **2002**, *41*, 1488−1508.

(3) Schneider, H.-J. Binding Mechanisms in Supramolecular Complexes. *Angew. Chem., Int. Ed.* **2009**, *48*, 3924−3977.

(4) Ghosh, I.; Nau, W. M. The Strategic Use of Supramolecular pKa Shifts To Enhance the Bioavailability of Drugs. *Adv. Drug Delivery Rev.* **2012**, *64*, 764−783.

(5) Márquez, C.; Hudgins, R. R.; Nau, W. M. Mechanism of Host−Guest Complexation by Cucurbituril. *J. Am. Chem. Soc.* **2004**, *126*, 5806−5816.

(6) Lee, J. W.; Samal, S.; Selvapalam, N.; Kim, H.-J.; Kim, K. Cucurbituril Homologues and Derivatives: New Opportunities in Supramolecular Chemistry. *Acc. Chem. Res.* **2003**, *36*, 621−630.

(7) Lagona, J.; Mukhopadhyay, P.; Chakrabarti, S.; Isaacs, L. The Cucurbit[n]uril Family. *Angew. Chem., Int. Ed.* **2005**, *44*, 4844−4870.

(8) Koner, A. L.; Nau, W. M. Cucurbituril Encapsulation of Fluorescent Dyes. *Supramol. Chem.* **2007**, *19*, 55−66.

(9) Bhasikuttan, A. C.; Pal, H.; Mohanty, J. Cucurbit[n]uril Based Supramolecular Assemblies: Tunable Physico-Chemical Properties and Their Prospects. *Chem. Commun.* **2011**, *47*, 9959−9971.

(10) Masson, E.; Ling, X.; Joseph, R.; Kyeremeh-Mensah, L.; Lu, X. Cucurbituril Chemistry: A Tale of Supramolecular Success. *RSC Adv.* **2012**, *2*, 1213−1247.

(11) Shaikh, M.; Mohanty, J.; Bhasikuttan, A. C.; Uzunova, V. D.; Nau, W. M.; Pal, H. Salt-Induced Guest Relocation from a Macrocyclic Cavity into a Biomolecular Pocket: Interplay between Cucurbit[7]uril and Albumin. *Chem. Commun.* **2008**, 3681−3683.

(12) Dsouza, R. N.; Pischel, U.; Nau, W. M. Fluorescent Dyes and Their Supramolecular Host/Guest Complexes with Macrocycles in Aqueous Solution. *Chem. Rev.* **2011**, *111*, 7941−7980.

(13) Bakirci, H.; Nau, W. M. Fluorescence Regeneration as a Signaling Principle for Choline and Carnitine Binding: A Refined Supramolecular Sensor System Based on a Fluorescent Azoalkane. *Adv. Funct. Mater.* **2006**, *16*, 237−242.

(14) Ko, Y. H.; Kim, E.; Hwang, I.; Kim, K. Supramolecular Assemblies Built with Host-Stabilized Charge-Transfer Interactions. *Chem. Commun.* **2007**, 1305−1315.

(15) Pischel, U.; Uzunova, V. D.; Remon, P.; Nau, W. M. Supramolecular Logic with Macrocyclic Input and Competitive Reset. *Chem. Commun.* **2010**, *46*, 2635−2637.

(16) Mohanty, J.; Nau, W. M. Ultrastable Rhodamines with Cucurbituril. *Angew. Chem., Int. Ed.* **2005**, *44*, 3750−3754.
(17) Nau, W. M.; Mohanty, J. Taming Fluorescent Dyes with Cucurbituril. *Int. J. Photoenergy* **2005**, *7*, 133−141.
(18) Singleton, M. L.; Reibenspies, J. H.; Darensbourg, M. Y. A Cyclodextrin Host/Guest Approach to a Hydrogenase Active Site Biomimetic Cavity. *J. Am. Chem. Soc.* **2010**, *132*, 8870−8871.
(19) Pluth, M. D.; Bergman, R. G.; Raymond, K. N. Acid Catalysis in Basic Solution: A Supramolecular Host Promotes Orthoformate Hydrolysis. *Science* **2007**, *316*, 85−88.
(20) Jeon, Y. J.; Kim, S.-Y.; Ko, Y. H.; Sakamoto, S.; Yamaguchi, K.; Kim, K. Novel Molecular Drug Carrier: Encapsulation of Oxaliplatin in Cucurbit[7]uril and Its Effects on Stability and Reactivity of the Drug. *Org. Biomol. Chem.* **2005**, *3*, 2122−2125.
(21) Saleh, N.; Koner, A. L.; Nau, W. M. Activation and Stabilization of Drugs by Supramolecular pKa Shifts: Drug-Delivery Applications Tailored for Cucurbiturils. *Angew. Chem., Int. Ed.* **2008**, *47*, 5398−5401.
(22) Ghale, G.; Ramalingam, V.; Urbach, A. R.; Nau, W. M. Determining Protease Substrate Selectivity and Inhibition by Label-Free Supramolecular Tandem Enzyme Assays. *J. Am. Chem. Soc.* **2011**, *133*, 7528−7535.
(23) Dutta Choudhury, S.; Mohanty, J.; Pal, H.; Bhasikuttan, A. C. Cooperative Metal Ion Binding to a Cucurbit[7]uril-Thioflavin T Complex: Demonstration of a Stimulus-Responsive Fluorescent Supramolecular Capsule. *J. Am. Chem. Soc.* **2010**, *132*, 1395−1401.
(24) Frampton, M. J.; Anderson, H. L. Insulated Molecular Wires. *Angew. Chem., Int. Ed.* **2007**, *46*, 1028−1064.
(25) Mohanty, J.; Bhasikuttan, A. C.; Dutta Choudhury, S.; Pal, H. Noncovalent Interaction of 5,10,15,20-Tetrakis(4-*N*-methylpyridyl)-porphyrin with Cucurbit[7]uril: A Supramolecular Architecture. *J. Phys. Chem. B* **2008**, *112*, 10782−10785.
(26) Angelos, S.; Yang, Y.-W.; Patel, K.; Stoddart, J. F.; Zin, J. I. pH-Responsive Supramolecular Nanovalves Based on Cucurbit[6]uril Pseudorotaxanes. *Angew. Chem., Int. Ed.* **2008**, *47*, 2222−2226.
(27) Pluth, M. D.; Bergman, R. G.; Raymond, K. N. Making Amines Strong Bases: Thermodynamic Stabilization of Protonated Guests in a Highly-Charged Supramolecular Host. *J. Am. Chem. Soc.* **2007**, *129*, 11459−11467.
(28) Rauwald, U.; Barrio, J.; Loh, X. J.; Scherman, O. A. "on-Demand" Control of Thermoresponsive Properties of Poly(*N*-isopropylacrylamide) with Cucurbit[8]uril Host−Guest Complexes. *Chem. Commun.* **2011**, *47*, 6000−6002.
(29) Mohanty, J.; Dutta Choudhury, S.; Upadhyaya, H. P.; Bhasikuttan, A. C.; Pal, H. Control of the Supramolecular Excimer Formation of Thioflavin T within a Cucurbit[8]uril Host: A Fluorescence on/off Mechanism. *Chem.—Eur. J.* **2009**, *15*, 5215−5219.
(30) Ghale, G.; Ramalingam, V.; Urbach, A. R.; Nau, W. M. Determining Protease Substrate Selectivity and Inhibition by Label-Free Supramolecular Tandem Enzyme Assays. *J. Am. Chem. Soc.* **2011**, *133*, 7528−7535.
(31) Park, C.; Kim, H.; Kim, S.; Kim, C. Enzyme Responsive Nanocontainers with Cyclodextrin Gatekeepers and Synergistic Effects in Release of Guests. *J. Am. Chem. Soc.* **2009**, 16614−16615.
(32) Shaikh, M.; Dutta Choudhury, S.; Mohanty, J.; Bhasikuttan, A. C.; Nau, W. M.; Pal, H. Modulation of Excited-State Proton Transfer of 2-(2′-Hydroxyphenyl)benzimidazole in a Macrocyclic Cucurbit[7]-uril Host Cavity: Dual Emission Behavior and $pK_a$ Shift. *Chem.—Eur. J.* **2009**, *15*, 12362−12370.
(33) Barooah, N.; Mohanty, J.; Pal, H.; Bhasikuttan, A. C. Stimulus-Responsive Supramolecular pKa Tuning of Cucurbit[7]uril Encapsulated Coumarin 6 Dye. *J. Phys. Chem. B* **2012**, *116*, 3683−3689.
(34) Jones-II, G.; Jackson, W. R.; Kanoktanaporn, S.; Halpern, A. M. Solvent Effects on Photophysical Parameters for Coumarin Laser Dyes. *Opt. Commun.* **1980**, *33*, 315−320.
(35) Jones-II, G.; Jackson, W. R.; Halpern, A. M. Medium Effects on Fluorescence Quantum Yields and Lifetimes for Coumarin Laser Dyes. *Chem. Phys. Lett.* **1980**, *72*, 391−395.
(36) Jones-II, G.; Jackson, W. R.; Choi, C.-y.; Bergmark, W. R. Solvent Effects on Emission Yield and Lifetime for Coumarin Laser Dyes. Requirements for a Rotatory Decay Mechanism. *J. Phys. Chem.* **1985**, *89*, 294−300.
(37) Madhavan, G. R.; Balraju, V.; Mallesham, B.; Chakrabarti, R.; Lohray, V. B. Novel Coumarin Derivatives of Heterocyclic Compounds as Lipid-Lowering Agents. *Bioorg. Med. Chem. Lett.* **2003**, *13*, 2547−2551.
(38) Signore, G.; Nifosi, R.; Albertazzi, L.; Storti, B.; Bizzarri, R. Polarity-Sensitive Coumarins Tailored to Live Cell Imaging. *J. Am. Chem. Soc.* **2010**, *132*, 1276−1288.
(39) Satpati, A. K.; Kumbhakar, M.; Nath, S.; Pal, H. Photophysical Properties of Coumarin-7 Dye: Role of Twisted Intramolecular Charge Transfer State in High Polarity Protic Solvents. *Photochem. Photobiol.* **2009**, *85*, 119−129.
(40) Jones-II, G.; Jimenez, J. A. C. Azole-Linked Coumarin Dyes as Fluoresence Probes of Domain-Forming Polymers. *J. Photochem. Photobiol., B* **2001**, *65*, 5−12.
(41) Klymchenko, A. S.; Demchenko, A. P. Electrochromic Modulation of Excited-State Intramolecular Proton Transfer: The New Principle in Design of Fluorescence Sensors. *J. Am. Chem. Soc.* **2002**, *124*, 12372−12379.
(42) Wagner, B. D. The Use of Coumarins as Environmentally-Sensitive Fluorescent Probes of Heterogeneous Inclusion Systems. *Molecules* **2009**, *14*, 210−237.
(43) Vasylevska, A. S.; Karasyov, A. A.; Borisov, S. M.; Krause, C. Novel Coumarin-Based Fluorescent pH Indicators, Probes and Membranes Covering a Broad pH Range. *Anal. Bioanal. Chem.* **2007**, *387*, 2131−2141.
(44) Lee, M.-T.; Yen, C.-K.; Yang, W.-P.; Chen, H.-H.; Liao, C.-H.; Tsai, C.-H.; Chen, C. H. Efficient Green Coumarin Dopants for Organic Light-Emitting Devices. *Org. Lett.* **2004**, No. 8, 1241−1244.
(45) Swanson, S. A.; Wallraff, G. M.; Chen, J. P.; Zhang, W.; Bozano, L. D.; Carter, K. R.; Salem, J. R.; Villa, R.; Scott, J. C. Stable and Efficient Fluorescent Red and Green Dyes for External and Internal Conversion of Blue OLED Emission. *Chem. Mater.* **2003**, *15*, 2305−2312.
(46) Jones, G., II; Jimenez, J. A. C. Intramolecular Photoinduced Electron Transfer for Cations Derived from Azol-Substituted Coumarin Dyes. *Tetrahedron Lett.* **1999**, *40*, 8551−8555.
(47) Marquez, C.; Huang, F.; Nau, W. M. Cucurbiturils: Molecular Nanocapsules for Time-Resolved Fluorescence-Based Assays. *IEEE Trans. Nanobiosci.* **2004**, *3*, 39−45.
(48) Valeur, B. *Molecular Fluorescence: Principles and Applications*; Wiley-VCH Verlag GmbH: Weinheim, Germany, 2002.
(49) Lakowicz, J. R. *Principles of Fluorescence Spectroscopy*, 3rd ed.; Springer Science+Business Media, LLC: New York, U.S., 2006.
(50) Glasoe, P. K.; Long, F. A. Use of Glass Electrodes To Measure Acidities in Deutrium Oxide. *J. Phys. Chem.* **1960**, *64*, 188−190.
(51) Perdew, J. P. Density-Functional Approximation for the Correlation Energy of the Inhomogeneous Electron Gas. *Phys.Rev. B* **1986**, *33*, 8822−8824.
(52) Becke, A. D. Density-Functional Exchange-Energy Approximation with Correct Asymptotic Behavior. *Phys. Rev. A* **1988**, *38*, 3098−3100.
(53) Schäfer, A.; Horn, H.; Ahlrichs, R. Fully Optimized Contracted Gaussian Basis Sets for Atoms Li to Kr. *J. Chem. Phys.* **1992**, *97*, 2571−2577.
(54) Lee, C.; Yang, W.; Parr, R. G. Development of the Colle−Salvetti Correlation-Energy Formula into a Functional of the Electron Density. *Phys. Rev. B* **1988**, *37*, 785−789.
(55) Becke, A. D. Density-Functional Thermochemistry. III. The Role of Exact Exchange. *J. Chem. Phys.* **1993**, *98*, 5648−5682.
(56) Schäfer, A.; Huber, C.; Ahlrichs, R. Fully Optimized Contracted Gaussian Basis Sets of Triple Zeta Valence Quality for Atoms Li to Kr. *J. Chem. Phys.* **1994**, *100*, 5829−5835.
(57) Weigend, F.; Ahlrichs, R. Balanced Basis Sets of Split Valence, Triple Zeta Valence and Quadruple Zeta Valence Quality for H to Rn:

Design and Assessment of Accuracy. *Phys. Chem. Chem. Phys.* **2005**, *7*, 3297−3305.
(58) Shaikh, M.; Mohanty, J.; Sundararajan, M.; Bhasikuttan, A. C.; Pal, H. Supramolecular Host−Guest Interactions of Oxazine-1 Dye with $\beta$- and $\gamma$-Cyclodextrins: A Photophysical and Quantum Chemical Study. *J. Phys. Chem. B* **2012**, *116*, 12450−12459.
(59) *TURBOMOLE*, version 6.3; TURBOMOLE GmbH: Karlsruhe, Germany, 2011; available at http://www.turbomole.com.
(60) Barooah, N.; Mohanty, J.; Pal, H.; Bhasikuttan, A. C. Non-Covalent Interactions of Coumarin Dyes with Cucurbit[7]uril Macrocycle: Modulation of ICT to TICT State Conversion. *Org. Biomol. Chem.* **2012**, *10*, 5055−5062.
(61) Dahiya, P.; Kumbhakar, M.; Mukherjee, T.; Pal, H. Effect of Protic Solvents on Twisted Intramolecular Charge Transfer State Formation in Coumarin-152 and Coumarin-481 Dyes. *Chem. Phys. Lett.* **2005**, *414*, 148−154.
(62) Satpati, A. K.; Kumbhakar, M.; Nath, S.; Pal, H. Photophysical Properties of Coumarin-7 Dye: Role of Twisted Intramolecular Charge Transfer State in High Polarity Protic Solvents. *Photochem. Photobiol.* **2009**, *85*, 119−129.
(63) Senthilkumar, S.; Nath, S.; Pal, H. Photophysical Properties of Coumarin-30 Dye in Aprotic and Protic Solvents of Varying Polarities. *Photochem. Photobiol.* **2004**, *80*, 104−111.
(64) Khorwal, V.; Sadhu, B.; Dey, A.; Sundararajan, M.; Datta, A. Modulation of Protonation−Deprotonation Processes of 2-(4′-Pyridyl)benzimidazole in Its Inclusion Complexes with Cyclodextrins. *J. Phys. Chem. B* **2013**, *117*, 8603−8610.